Published in final edited form as:
Biomaterials. 2010 May ; 31(14): 4146–4156. doi:10.1016/j.biomaterials.2010.01.112.

Antibiotic-releasing Porous Polymethylmethacrylate Constructs for Osseous Space Maintenance and Infection Control

Meng Shi[1], **James D. Kretlow**[1], **Anson Nguyen**[2], **Simon Young**[1,3], **L. Scott Baggett**[4], **Mark E. Wong**[3], **F. Kurtis Kasper**[1], and **Antonios G. Mikos**[1,*]

[1]Department of Bioengineering, Rice University, Houston, TX USA

[2]School of Medicine, University of Texas Medical Branch at Galveston, Galveston, TX USA

[3]Department of Oral and Maxillofacial Surgery, University of Texas Health Science Center at Houston, Houston, TX USA

[4]Department of Statistics, Rice University, Houston, TX USA

Abstract

The use of a strategy involving space maintenance as the initial step of a two-stage regenerative medicine approach toward reconstructing significant bony or composite tissue defects in the craniofacial area, preserves the void volume of bony defects and could promote soft tissue healing prior to the subsequent definitive repair. One of the complications with a biomaterial-based space maintenance approach is local infection, which requires early, effective eradication, ideally through local antibiotic delivery. The purpose of this study is to develop a dual function implant material for maintaining osseous space and releasing an antibiotic to eliminate local infection in bony defects. Colistin, a polymyxin antibiotic, was chosen specifically to address infections with *Acinetobacter* species, the most common pathogen associated with combat-related traumatic craniofacial injuries. Porous polymethylmethacrylate (PMMA) constructs incorporating poly(lactic-*co*-glycolic acid) (PLGA) microspheres were fabricated by mixing a clinically used bone cement formulation of PMMA powder and methylmethacrylate liquid with a carboxymethylcellulose (CMC) hydrogel (40 or 50 wt%) to impart porosity and PLGA microspheres (10 or 15 wt%) loaded with colistin to control drug release. The PMMA/CMC/PLGA construct featured mild setting temperature, controllable surface/bulk porosity by incorporation of the CMC hydrogel, reasonably strong compressive properties, and continuous drug release over a period of 5 weeks with total drug release of 68.1-88.3%, depending on the weight percentage of CMC and PLGA incorporation. The concentration of released colistin was well above its reported minimum inhibitory concentration against susceptible species for 5 weeks. This study provides information on the composition parameters that enable viable porosity characteristics/drug release kinetics of the PMMA/CMC/PLGA construct for the initial space maintenance as part of a two-stage regenerative medicine approach.

*Corresponding Author: Antonios G. Mikos, Ph.D., Rice University, Department of Bioengineering – MS 142, P.O. Box 1892, Houston, Texas 77251-1892, Tel.: +1 713 348 5355; Fax: +1 713 348 4244, mikos@rice.edu.

Paper submitted to *Biomaterials*

Keywords

Bone tissue engineering; Scaffolds; Biodegradable microspheres; Polymethylmethacrylate; Carboxymethylcellulose; Colistin

1. Introduction

Craniofacial trauma is among the most debilitating forms of injury facing civilian and military populations due to the important aesthetic and functional role of the craniofacial complex [1, 2]. Blast injuries and injuries from high velocity projectiles (e.g., those encountered on the battlefield) often require a staged repair where the surgical revision, however, is sometimes complicated by distortion of surgical landmarks, diminished volume of the defect space, fibrosis of the tissue bed and/or local contamination [3-8]. Over the course of a staged reconstruction, the placement of a temporary, alloplastic implant may eliminate many of the aforementioned complications [9,10]. Toward treating traumatic craniofacial injuries with significant bone/tissue loss, our laboratory is developing a two-stage regenerative medicine approach consisting of a first stage using temporary space maintenance to not only maintain the void space but also to prime the wound site for later definitive reconstruction [10]. The initial space maintenance using a non-biodegradable implant material (i.e., a space maintainer) preserves the original dimensions of the bony defects and prevents soft tissue ingrowth while, importantly, allowing for wound/tissue healing over the material. Successful space maintenance creates a soft tissue envelope with definitely preserved volume and well-healed surrounding tissues, ideal for the placement of a tissue engineering construct designed for bone regeneration during the subsequent reconstruction stage [9-12]. In order to advance the development of this two-stage regenerative medicine approach, we herein designed a polymethylmethacrylate (PMMA)-based space maintainer featuring a porous structure to promote wound/tissue healing over the material and implant retention at the host site [10]. In addition, an antibiotic delivery system is incorporated to mitigate/prevent local infections, thereby reducing the potential for any infection-related complication associated with space maintenance.

Self-hardening PMMA cement has been successfully used in a variety of orthopaedic conditions because of its appealing physical and chemical characteristics [13,14]. The non-degradability allows PMMA constructs to maintain sufficient mechanical support over an extended time period. It can also be molded intraoperatively to fill complex defects, making PMMA implants particularly suited for osseous space maintenance in oral and craniofacial reconstructions [9,15-17]. While conventional PMMA cement has been previously used in space maintenance applications, problems with implant extrusion or wound dehiscence have been reported [10,11,18]. It has been demonstrated that the porous structure of an implant material plays an essential role in anchoring the material to the host by allowing for rapid ingrowth of fibrovascular and soft tissue into the pores to promote wound healing and the formation of a stable interface [10,18-22]. A porous PMMA structure thus becomes the gold standard for designing an effective space maintainer in the envisioned two-stage approach.

Infections following traumatic injuries, including combat wound infections and osteomyelitis, are a common occurrence [7,8,23-25]. Latent or active posttraumatic and postsurgical infections may potentially hinder wound healing and tissue regeneration, underscoring the importance of effective, early eradication/prevention by antibiotic drugs. The multidrug-resistant (MDR) *Acinetobacter baumannii* species has been demonstrated to be the predominant organism recovered in trauma-related infections sustained by US soldiers in Iraq and Afghanistan [24-26]. Colistin, one of the last-resort antibiotics for this species, holds promise as an effective antimicrobial agent [27-30]. The parenteral administration of colistin

requires a long course of therapy due to the poor penetration of the antibiotic into bone. Long-term parenteral colistin administration is associated with a high incidence of nephrotoxicity and neurotoxicity [28,30], whereas a local delivery of antibiotic drugs promises to achieve local therapeutic drug levels over an extended duration while eliminating systemic exposure to potentially toxic drug concentrations [31-33]. Consequently, the development of a local antibiotic delivery system delivered through an implant becomes a potentially important strategy in space maintenance.

Building upon the advantages of a porous implant structure to improve incorporation into the surrounding tissue bed through the incorporation of controlled drug delivery to address local infections, a space maintainer was designed as a poly(lactic-*co*-glycolic acid) (PLGA) microsphere-incorporating porous PMMA construct. The antibiotic drug colistin was first loaded into biodegradable PLGA microspheres, and the PLGA microspheres were then mixed with the PMMA cement, while a carboxymethylcellulose (CMC) hydrogel component was co-incorporated to impart porosity throughout the constructs [10,21,34]. All components in these PMMA/CMC/PLGA constructs are regulated by the United States Food and Drug Administration (FDA) for orthopaedic and/or craniofacial applications. A construct successfully developed from this combination has the potential to transition readily from experimental research into clinical use.

The aim of the present *in vitro* study was to elucidate the influence of material composition of PMMA/CMC/PLGA constructs on their physical properties and provide predictive insight into the expected space maintenance and drug delivery capability of the space maintainer over time *in vivo*. Specifically, it was hypothesized that the overall porosity would be tailored by the incorporation of CMC hydrogel and would not be significantly changed with the addition of PLGA microspheres. The incorporation of PLGA microspheres in porous PMMA constructs was hypothesized to allow for a sustained, high concentration colistin release over weeks. To test these hypotheses, four formulations of PMMA/CMC/PLGA constructs with 40-50 wt% CMC and 10-15 wt% PLGA microsphere incorporation were investigated for surface and bulk morphology, porosity, pore interconnectivity and compressive mechanical properties initially and throughout a degradation process of 12 weeks. *In vitro* drug release kinetics were also examined over a period of 5 weeks.

2. Materials and methods

2.1 Materials

Poly(lactic-*co*-glycolic acid) (PLGA) (copolymer ratio of 50:50, weight average molecular weight of 61.1 kDa and number average molecular weight of 37.3 kDa as determined by gel permeation chromatography based on polystyrene standards) was purchased from Lakeshore Biomaterials (Birmingham, AL). Colistin sulfate salt was purchased from Sigma-Aldrich (St. Louis, MO). PMMA cement (SmartSet®, High Viscosity) was from DePuy Orthopaedics Inc. (Warsaw, IN). Carboxymethylcellulose sodium was purchased from Spectrum® chemical MFG Corp. (Gardena, CA). Poly(vinyl alcohol) (PVA) (88% hydrolyzed, nominal molecular weight 22 kDa) was from Acros Organics (Geel, Belgium). All other reagents were purchased from Sigma-Aldrich (St. Louis, MO) and used as received.

2.2 Preparation of colistin-loaded PLGA microspheres

Colistin-loaded PLGA microspheres were fabricated by a water-in-oil-in-water (W/O/W) double emulsion solvent evaporation technique [35]. Briefly, PLGA polymer (2.0 g) was dissolved in methylene chloride at a concentration of 50 mg/mL as an oil phase, and colistin (650 mg) was dissolved in 2 mL distilled water (internal aqueous phase) containing 0.4 wt% PVA. The colistin solution was dispersed in the polymer solution by a homogenizer (PRO250,

Pro Scientific Inc., Monroe, CT) at 26,000 rpm for 30 s. This stable W/O emulsion was slowly added into an aqueous solution (external aqueous phase, 400 mL) containing 0.4 wt% PVA and 0.5 M NaCl under stirring at 500 rpm and the solution was stirred at 500 rpm for 30 min. Solvent removal and microsphere hardening was achieved by stirring at 300 rpm for another 3.5 h. The microspheres were isolated by centrifugation, washed with distilled water three times, and then vacuum-dried for 24 h.

The drug content in the PLGA microspheres was determined by first dissolving microspheres in methylene chloride and then extracting colistin with phosphate buffered saline (PBS) buffer (pH 7.4). Briefly, 20 mg colistin-loaded microspheres were dissolved in 1 mL methylene chloride and then 20 mL PBS was added to the solution. The solution mixture was vigorously stirred for 2 h allowing for the extraction of colistin by the aqueous phase and evaporation of the organic solution.

The colistin concentration in the PBS buffer was analyzed by high-performance liquid chromatography (HPLC) (Waters®, Milford, MA) [36]. The HPLC system consisted of a Waters 2695 separation module and a 2996 photodiode array (PDA) detector. The separation was performed using an XTerra® RP 18 column (250 cm × 4.6 μm, Waters®) at a column temperature of 45°C and a flow rate of 0.5 mL/min in a mobile phase consisting of acetonitrile (HPLC grade with 0.1 vol% trifluoroacetic acid) and water (HPLC grade with 0.1 vol% trifluoroacetic acid). Peaks were eluted with a linear gradient of 10–65% acetonitrile in water over 20 min. Absorbance was monitored at $\lambda = 214$ nm. The two main components colistin A and colistin B were eluted at approximately 14.9 min and 15.7 min, respectively. Standard solutions with colistin in PBS buffer (pH 7.4) were tested in the range of 5–1000 μg/mL. Calibration curves were obtained using the combined peak areas of colistin A and colistin B versus the colistin concentration.

2.3 Preparation of microsphere-incorporating porous PMMA constructs

Antibiotic-releasing porous PMMA constructs were fabricated by mixing a clinical grade bone cement formulation of PMMA powder and MMA liquid with a CMC hydrogel and colistin-loaded PLGA microspheres. The percentage of PLGA microspheres was varied (10 wt% or 15 wt%) to adjust the drug content in each volume unit of the construct. The percentage of CMC hydrogel was varied (40 wt% or 50 wt%) to control the surface/bulk porosity of the constructs (Table 1). The CMC hydrogel was prepared by dissolving carboxymethylcellulose sodium (9 wt%) in distilled water, which resulted in a highly viscous hydrogel [10]. The following mixing procedure was employed to provide the most reproducible and homogeneous distribution of hydrogel phase according to previous experience: first the PMMA powder and the PLGA microspheres that were needed for 10 or 15 wt% relative to the polymer phase (PLGA+PMMA +MMA) were fully mixed using a spatula. Then the powder mixture was dispersed in a predetermined weight of CMC hydrogel (40 or 50 wt% in the constructs of CMC+PLGA +PMMA+MMA) by manual stirring. The monomer liquid was added into the mixture and the two phases were mixed carefully to ensure uniform distribution of the monomer while minimizing air entrapment. After the mixture reached a dough-like consistency (approximately 90 s), the mixture was subsequently inserted into Teflon molds. The cement mixtures were allowed to harden in the molds for 30 min at ambient temperature (21°C). After the removal of constructs from the molds, the constructs were vacuum-dried overnight.

Cylinders 6 mm in diameter and 12 mm in height were used for mechanical testing based on the International Organization for Standardization Standard ISO5833 [37]. Cylinders 10 mm in diameter and 6 mm in height, which were designed for a previously developed rabbit mandibular defect model [10,38] were used for the degradation study/*in vitro* drug release.

2.4 Scanning electron microscopy (SEM)

SEM was employed to examine the external and internal morphology of colistin-loaded PLGA microspheres and the surface roughness and porosity of microsphere-incorporating constructs. The microspheres or the surface of constructs were sputter-coated with gold for 40 s at 100 mA using a CrC-150 sputtering system (Torr International, New Windsor, NY) and observed under a FEI Quanta 400 field emission scanning electron microscope (FEI company, Hillsboro, OR) at an accelerating voltage of 10 kV.

2.5 Setting temperature and time

Setting temperature and time were measured simultaneously by recording the temperature of the cement mixture as a function of time after the addition of the last component. According to ISO5833 for acrylic resin cements [37], the dough-like mixture was packed into a Teflon cylindrical mold (60 mm in diameter, 6 mm in height) where a temperature measurement probe connected to a multimeter (Datalogging Multimeter, Data Acquisition System ML720, Extech Instruments Corp., MA) was positioned in the center of the mold to record the temperature of the mixture every 0.2 s until the temperature began to drop. The setting temperature was calculated as:

$$T_{set} = (T_{max} + T_{amb})/2$$

where T_{max} is the highest temperature attained during polymerization, and T_{amb} is the recorded ambient temperature.

For each measurement, the temperature change was plotted against time and the setting time t_{set} was measured from the beginning of mixing until the temperature reached the setting temperature T_{set}. The average and standard deviation of T_{set} and t_{set} were determined from three measurements.

2.6 Microcomputed tomography (microCT)

A SkyScan 1172 microCT imaging system (Aartselaar, Belgium) was used to perform nondestructive imaging and quantify the 3D microarchitectural morphology of original and degraded constructs. The samples (n=3) were imaged with an X-ray tube voltage of 40 kV and current of 250 mA without a filter. Volumetric reconstruction and analysis were conducted using the software NRecon and CTAn provided by SkyScan. The images obtained from acquisition were first reconstructed to serial coronal-oriented tomograms using a 3D cone beam reconstruction algorithm and then segmented into binary images using adaptive local thresholding to distinguish polymer material from pore space and to eliminate background noise. An optimal threshold value of 60-255 was applied for all 3D reconstructions and quantitative analyses. Representative 3D reconstructions of constructs were generated based on the binarized tomograms to visually show the 3D models of microstructures of scaffolds. To quantitatively analyze the porosity and interconnectivity, a cylindrical volume of interest (VOI) 5.8 mm in diameter and 9.8 mm in height was selected in order to eliminate potential edge effects. The bulk porosity of constructs was calculated as:

Bulk porosity = 100%-vol% of binarized object in VOI

The interconnectivity was quantified as the fraction of the pore volume in a construct that was accessible from the outside through openings of a certain minimum size (a sphere diameter of 40-160 μm). A shrink-wrap process was performed to shrink the outside boundary of the VOI in a construct through any openings where the spheres could pass, and the total volume of the VOI (V) and the volume of the binarized object ($V_{shrink\text{-}wrap}$) were measured. If 100% of the porosity was accessible to the sphere, then $V = V_{shrink\text{-}wrap}$; otherwise, $V_{shrink\text{-}wrap} < V$ because

the volume of the VOI includes the volume of the construct plus any void space that is not accessible. Interconnectivity was calculated as follows:

$$\text{Interconnectivity} = (V\text{-}V_{shrink\text{-}wrap})/(V\text{-}V_m) \times 100\%$$

where V is the total volume of the VOI, $V_{shrink\text{-}wrap}$ is the VOI volume after shrink-wrap processing, and V_m is the volume of construct materials.

2.7 Compressive modulus and strength

The compressive mechanical properties of microsphere-incorporating constructs were measured to establish the influence of CMC/PLGA incorporation on mechanical performance. In accordance with ISO5833, 6 mm × 12 mm cylindrical constructs (n=6) were compressed along their long axis at a cross-head speed of 20 mm/min using a mechanical testing machine (MTS, 858 Mini Bionix, Eden Prairie, MN) with a 10 kN load cell.

Constructs (cylinders of 10 mm in diameter, 6 mm in height) that were designed for a mandibular defect model [10,38] were used in the degradation study. Although these dimensions do not conform to ISO specifications, the mechanical testing over time of these degraded constructs was performed to provide insight on the change of mechanical performance over time *in vivo*. The degraded cylindrical constructs (n=3) were compressed along their long axis at a cross-head speed of 1 mm/min with a 10 kN load cell (MTS).

For both compressive tests, force and displacement were recorded throughout the compression and converted to stress and strain based on the initial specimen dimensions. The compressive modulus was analyzed using the TestStar 790.90 mechanical data analysis package designed by MTS and calculated as the slope of the initial linear portion of the stress-strain curve. The offset compressive yield strength was determined as the stress at which the stress-strain curve intersected with a line drawn parallel to the slope defining the modulus, beginning at 2.0% strain (based on ISO5833) [37].

2.8 *In vitro* drug release

The *in vitro* drug release study was carried out in triplicate at 37°C in PBS buffer (pH 7.4). Each construct was incubated in 5 mL PBS buffer under mild shaking. At predetermined time intervals, the release medium from each sample was completely removed and replaced with fresh PBS buffer. The release medium was filtered with a 0.2 μm filter and tested by HPLC to determine the colistin concentration. The HPLC method is described above in Section 2.2. The cumulative release (%) was expressed as the percent of total colistin released over time. The daily release of colistin was calculated from the absolute amount of colistin released between three or four consecutive days divided by the corresponding release time as well as the construct volume, and was expressed as μg colistin/mL construct/day.

2.9 Statistical analysis

For porosity, setting temperature and time, and compressive modulus data, statistical analysis was performed with a single-factor analysis of variance (ANOVA) with a 95% confidence interval ($p<0.05$). In the case of statistically significant differences, Tukey's *post hoc* test was conducted. For comparing the cumulative release data in the *in vitro* colistin release study, a repeated measures analysis of variance was performed, followed by a Tukey's multiple comparison test to determine statistical significance at an alpha level of 0.05. The comparison of the first day release of constructs with PLGA microspheres and the pairwise comparison of the release rate of sustained release period (phase 3) of constructs were performed with a single-factor analysis of variance followed by a Tukey's multiple comparison test. Data are presented as means ± standard deviation.

3. Results

3.1 Colistin-loaded PLGA microspheres

The ability of PLGA microspheres to control colistin release was first examined. Colistin-loaded PLGA microspheres with a 16.1±2.5 wt% drug loading were prepared by a water-in-oil-in-water double emulsion method. The SEM images of external and internal morphologies (Figure 1 inset) showed spherically shaped microparticles with smooth surfaces and a highly porous internal polymeric matrix. The colistin-loaded PLGA microspheres exhibited a typical three-phase release profile (Figure 1), including an initial burst of 52.3±6.2% release at days 0-2, a lag phase characterized by a moderate drug release (0.9±0.2% per day at days 2-11), and a sustained, accelerated drug release (1.9±0.2% per day at days 11-25) lasting for two weeks. The PLGA microspheres alone exhibited a continuous colistin release over a period of 4 weeks with an 87.5±9.9% total colistin release.

3.2 Microsphere-incorporating PMMA/CMC/PLGA constructs

To prepare the microsphere-incorporating porous constructs, the PLGA microspheres were first mixed with the PMMA powder, and then the powder mixture was homogenously dispersed in the CMC hydrogel, followed by the addition of the MMA liquid phase. Curing of the mixture occurred when the initiator in the powder phase started polymerization of the reactive MMA monomer, thus trapping the PLGA microspheres, PMMA microparticles, and CMC hydrogel within the polymerizing matrix. The CMC hydrogel dispersed throughout the polymerizing matrix, yielding the initial surface/bulk porosity. The surface morphologies of dry construct samples were characterized by microCT and SEM (Figure 2). Higher CMC hydrogel incorporation (50 wt% versus 40 wt%) resulted in greater roughness and pore depth on the construct surface (Figure 2A and 2B). Importantly, the PLGA microspheres were homogeneously dispersed among the PMMA microparticles (the PLGA microspheres could not be distinguished from the PMMA particles in SEM images due to similar sizes) (Figure 2C). The PLGA microspheres and PMMA particles were more likely entrapped within the continuous polymer phase rather than localized inside the pores.

The temperature change during the setting process was monitored following ISO5833 for acrylic cements to elucidate the influence of CMC/PLGA addition on the setting temperatures and times. Due to the exothermic nature of the PMMA/MMA polymerization reaction, the temperature in the pure PMMA cement rapidly increased to 88.3±0.6°C. Notably, CMC hydrogel incorporation significantly reduced the maximum temperature of constructs (Figure 3 and Table 2). When incorporating CMC hydrogel alone, the maximum temperature was reduced to 43.7±2.1°C for the 40 wt% CMC incorporation and 36.3±1.2°C for the 50 wt% CMC incorporation (compared to 88.3±0.6°C for the solid PMMA) ($p<0.05$). Importantly, higher CMC incorporation resulted in significantly greater reduction in the maximum temperature ($p<0.05$). The addition of PLGA besides CMC further reduced the maximum temperature in the 15%PLGA-40%CMC construct (38.7±1.2°C versus 43.7±2.1°C for the 40 wt% CMC-incorporating construct without PLGA) ($p<0.05$), whereas it did not alter the maximum temperatures ($p>0.05$) in other constructs. The setting times of PMMA/CMC or PMMA/CMC/PLGA constructs were reduced ($p<0.05$) by the presence of CMC hydrogel and/or PLGA microspheres except in the construct with 50 wt% CMC incorporation alone (Table 2).

The compressive modulus and offset yield strength (2.0% offset) were determined based on ISO5833 (Figure 4). The compressive modulus of porous PMMA/CMC/PLGA constructs varied between 262±33 and 658±80 MPa depending on the amount of CMC incorporation, and was lower than that of solid PMMA (2666±218 MPa) ($p<0.05$). The compressive mechanical performance was affected by the amount of CMC hydrogel incorporation, with greater CMC

incorporation resulting in significantly lower compressive modulus (586±80-658±80 MPa for the 40 wt% CMC incorporation versus 262±33-313±41 MPa for the 50 wt% CMC incorporation) ($p<0.05$). The offset yield strength of PMMA/CMC/PLGA constructs presented a similar CMC-incorporation dependence ($p<0.05$).

3.3 Degradation behavior of PMMA/CMC/PLGA constructs

Construct formulations (cylinders 6 mm in height and 10 mm in diameter) that were designed for implantation within a recently developed rabbit mandibular defect model [10,38] were degraded over a period of 12 weeks *in vitro*, and the degradation process was characterized by the changes in the bulk porosity and pore interconnectivity (Figure 5) and compressive mechanical performance (Figure 6). The cross-sectional morphologies of constructs (Figure 5A) demonstrated significant porosity and interconnectivity among pores of constructs in the different degradation stages. Figure 5B and 5C illustrate the quantitative increase of porosity and interconnectivity over the degradation process of 12 weeks. The PMMA/CMC/PLGA constructs initially featured a relatively low bulk porosity (5.9±3.8-8.0±7.0% for the 40 wt% CMC incorporation and 14.7±5.4-20.8±0.9% for the 50 wt% CMC incorporation at day 0). The bulk porosity increased significantly after the first day of degradation in the construct 15% PLGA-40%CMC (17.6±2.4%), 10%PLGA-50%CMC (32.4±1.2%) and 15%PLGA-50% CMC (36.9±3.0%) ($p<0.05$), but did not change significantly in the construct 10%PLGA-40% CMC (12.1±3.9%) ($p>0.05$). The bulk porosity exhibited an increasing trend over the degradation process of 12 weeks, reaching a plateau of 20.7±0.6-26.1±3.8% and 46.5±2.7-53.9 ±1.3% for the 40 and 50 wt% CMC incorporation groups, respectively (Figure 5B). Notably, the formulations fabricated with greater CMC incorporation (50 wt%) possessed significantly higher porosity during the degradation process, and their porosity increased significantly after the 12 week degradation ($p<0.05$); nevertheless, with the same CMC incorporation, the constructs with 10 and 15 wt% PLGA incorporation possessed similar porosities at the various stages of degradation. Similar CMC-incorporation dependence was also found in the pore interconnectivity of PMMA/CMC/PLGA constructs (Figure 5C): the constructs with higher CMC hydrogel incorporation exhibited higher pore interconnectivity ($p<0.05$) at smaller minimum connection sizes after the first day degradation (the dependence of pore interconnectivity on CMC hydrogel incorporation at different degradation stages was similar; data not shown). For example, at 40 μm connection size, 62.0±4.8-72.6±3.8% of the pores inside the 50 wt% CMC-incorporating construct were interconnected through openings, whereas the interconnectivity in the construct with lower CMC incorporation was significantly less (20.5±7.9-29.8±7.2% at 40 μm connection size) ($p<0.05$).

Constructs of cylindrical form with dimensions of 6 mm in height and 10 mm in diameter were tested mechanically to determine the influence of CMC/PLGA degradation on compressive mechanical properties and to provide predictive insight into the expected mechanical performance of the constructs over time *in vivo* [10]. The compressive modulus declined to 39.4±0.7-77.0±6.5% of the original compressive modulus after the first day of degradation and 12.2±2.0-32.0±2.0% after 12 weeks (Figure 6). The decrease in compressive modulus after 12 weeks was significantly greater than that after the first day of degradation for the same construct ($p<0.05$). Notably, the construct with both higher CMC and PLGA incorporation (15% PLGA-50%CMC) processed the greatest reduction in compressive modulus after 12 weeks ($p<0.05$).

3.4 *In vitro* colistin release

A 35-day *in vitro* release study was conducted to characterize the release kinetics of colistin. The PMMA/CMC/PLGA constructs exhibited triphasic release profiles similar to PLGA microspheres: an initial burst (17.5±0.9-24.0±0.7% per day at days 0-2), moderate release lag phase (0.5±0.0-0.9±0.0% per day at days 2-15), and sustained release periods (0.6±0.1-3.4

±0.2% per day at days 15-28) (Figure 7A and Table 3). Incorporating PLGA microspheres into PMMA constructs significantly reduced the initial release at the first day (23.0±1.5-32.8±1.9% for the PMMA/CMC/PLGA constructs versus 45.9±2.9% for the PLGA microspheres) ($p<0.05$), whereas the lag phase lasted longer for the PMMA/CMC/PLGA constructs (days 2-15 for the PMMA/CMC/PLGA constructs versus days 2-11 for the PLGA microspheres). Notably, the colistin release from the PMMA/CMC/PLGA constructs continued for another week (phase 4) after the accelerated, sustained release phase (0.6±0.1-1.0±0.3% and 1.8 ±0.3-1.9±0.7% colistin release for the 40 and 50 wt% CMC-incorporating constructs, respectively, during the fifth week) versus little or no colistin release after 4 weeks for the PLGA microspheres alone. All PMMA/CMC/PLGA constructs achieved considerable colistin release after 5 weeks (68.1±3.3-88.3±5.8%). The constructs prepared with higher CMC incorporation featured significantly greater amounts of colistin release for the same PLGA incorporation (85.4±7.2-88.3±5.8% versus 68.1±3.3-70.7±5.5%) ($p<0.05$) (Table 3), whereas varying PLGA microsphere incorporation did not significantly alter the total drug release for the same CMC incorporation ($p>0.05$). In terms of the release rate at the sustained release phase 3, increasing either the CMC or the PLGA incorporation resulted in significantly higher release during this period ($p<0.05$) (Table 3).

Figure 7B presents the release rate of colistin (i.e., the average concentration of released colistin per day), providing insight into the immediate local drug concentration throughout the release period. The daily release varied in accordance with the colistin release rate at different release phases. During the release period of 5 weeks, the concentration of released colistin within/around the construct remained at a level much higher than or around 10 μg/mL. For example, at the lowest point of lag phase of day 15, the constructs released colistin at a concentration of 16.6±8.4-42.3±7.5 μg/mL.

4. Discussion

Space maintenance, as the initial stage of a two-stage regenerative medicine approach toward reconstructing large bony defects, is particularly attractive when immediate reconstruction is not indicated [9,10,39]. An implant with the desirable characteristics of PMMA with additional features such as improved incorporation into the surrounding tissue bed would be ideal. A porous PMMA structure induced by the CMC hydrogel addition was thus designed to promote tissue healing and material retention by allowing for tissue ingrowth into the pores [10]. Furthermore, given the increasing trend in combat related *Acinetobacter* infections during recent military conflicts, a colistin releasing strategy was incorporated to mitigate infection-associated complications.

PLGA has been used for antibiotic delivery in the treatment of local infections either as a bone implant itself [40-42] or as the degradable component in composite implant materials [43]. The colistin release profile presented in Figure 1 illustrates a typical degradation-controlled release pattern [44]: the initial burst is the rapid release of surface-associated drugs; the lag phase of moderate drug release reflects the time necessary for PLGA hydrolysis to a critical chain length to allow dissolution and release of entrapped drug; and a sustained, accelerated drug release is followed where pore formation and fragmentation of the microspheres enhance erosion-accelerated drug release. To fabricate a colistin-releasing porous PMMA construct, CMC hydrogel and PLGA microspheres were co-incorporated into a clinically used PMMA cement. Physically mixing all components (PLGA microspheres, PMMA powder, CMC hydrogel and MMA monomer) prior to MMA polymerization is an appealing method that could be used intraoperatively to create a porous construct with PLGA microspheres homogeneously entrapped within the polymer phase (Figure 2). The aqueous CMC hydrogel micro-coalescences were dispersed throughout the curing material, creating a filament network (Figure 2). Resorption of the inclusions by the aqueous environment left voids forming the

pore structure [10,21,34] (Figure 5). The incorporation of CMC hydrogel created immediate surface/bulk porosity after fabrication. The degradation of PMMA/CMC/PLGA constructs (due to the dissolution of CMC and PLGA as well as any PMMA cement erosion upon contact of the construct with the aqueous/biological environment) generated further porosity throughout the constructs (Figure 5). By varying the PLGA and CMC composition, the PMMA/CMC/PLGA constructs featured both low (12.1±3.9-26.1±3.8% created by the 40 wt% CMC incorporation) and high (32.4±1.2-53.9±1.3% created by the 50 wt% CMC incorporation) porosity initially and throughout the degradation process, which matched the porosity of previously evaluated PMMA/CMC constructs (16.9% or 44.6% porosity), which improved oral mucosal healing as compared to non-porous PMMA over a clean/contaminated bone defect created in the rabbit mandible [10].

Besides imparting immediate porosity, an additional advantage offered through CMC incorporation was a substantial reduction of the setting temperature (Figure 3 and Table 2) [21,34]. The high temperature attained by exothermic polymerization of conventional PMMA cements has largely limited the types of antibiotics effectively incorporated into the cement. With the CMC hydrogel acting as an efficient heat sink and the CMC/PLGA addition “diluting” the polymerization (relatively less monomer polymerizes per unit volume), the PMMA/CMC/PLGA formulations produced maximum temperatures close to the physiological temperature of 37°C. This allows the loaded constructs to cure *in vivo* with little potential for thermal damage to sensitive antibiotic drugs or surrounding cells and tissues.

The creation of a porous structure, however, led to an expected and undesirable decline in the compressive mechanical properties relative to solid PMMA (Figure 4), in accordance with the typical porosity-mechanical property relationship in scaffold materials [34,45-49]. The decrease in compressive properties (262±33-658±80 MPa original compressive modulus; the compressive mechanical property declined further over time with construct degradation and subsequent bulk porosity increase) (Figure 4-6) presents a compromise if the construct is to be used for load-bearing applications, especially when long-term mechanical support (i.e., weeks or months) is required. For application in the craniofacial complex, porous PMMA constructs with significant porosity (50 vol%) remain useful in correcting craniofacial contour deformities and repairing defects in clinical applications [18,19,50], so even after 12 weeks of degradation (where the porosity of the PMMA/CMC/PLGA constructs did not exceed 50%), the PMMA/CMC/PLGA implants hold promise in providing support of craniomaxillofacial structures. In addition, the amount of CMC incorporation primarily determined the physical properties of the PMMA/CMC/PLGA constructs, making it feasible to tune the balance between porosity and subsequent drug release with the mechanical properties to meet a specific need of space maintenance/drug delivery.

In these PMMA/CMC/PLGA constructs, the original porosity and the porosity change over time would consequently impact the progressive tissue ingrowth (as in an *in vivo* environment), mechanical performance, and most importantly, drug elution through the open paths. The investigation of these properties throughout construct degradation will help to predict their capacity to allow tissue to integrate and correlate drug release kinetics with the porosity characteristics of the construct. As seen in Figure 5B, the significant increase in the bulk porosity after the first day of degradation could be mainly attributed to the rapid dissolution of CMC to the surrounding aqueous environment. This immediate porosity will be essential for the initial tissue ingrowth, since it is during the first 7 days after implantation that extensive invasion of vascularised fibrous connective tissue into surface pores occurs [18]. The continuous CMC/PLGA dissolution created further porosity over a period of 12 weeks (Figure 5B), which will potentially allow for the further integration of soft tissue or even the gradual ingrowth of hard tissue [18], promoting the formation of a stronger interface between the tissue and material. In addition, the development of the porosity was slow, which will help to prevent

early bacterial seeding of the implants, a development which potentially caused an inflammatory reaction in response to more porous formulations of PMMA/CMC implants tested *in vivo* in a clean/contaminated wound model [10].

Importantly, the surface/bulk porosity characteristics of PMMA/CMC/PLGA constructs was predominantly controlled by the CMC incorporation (Figure 5B) (i.e., the higher the CMC incorporation, the greater the surface/bulk porosity and pore interconnectivity). With respect to the concept of anchoring the constructs by tissue ingrowth into the surface pores, the degree of tissue ingrowth depends on the degree of surface porosity and dictates the strength of tissue-material interfaces [51]. The tunable surface/bulk porosity of the PMMA/CMC/PLGA constructs allows for the preparation of constructs with different degrees of porosity and the use of these constructs in applications at a wide range of sites where various strengths of the tissue-porous implant interface are expected.

The rapid dissolution of CMC yielded initial porosity and allowed fluid to penetrate into the inner phase of the construct to initiate PLGA hydrolysis and subsequent drug release. The CMC/PLGA dissolution generated more open paths, which largely benefited the drug elution from the inner structure of the constructs. The impact of bulk porosity and pore interconnectivity on the drug release was confirmed by the significantly higher drug release rate and total amount of released drug (Table 3) achieved by the constructs with 50 wt% CMC incorporation. The colistin release from the PMMA/CMC/PLGA constructs achieved a prolonged release duration (5 weeks) and significantly enhanced cumulative release (68.1 ±3.3-88.3±5.8%) (Figure 7A) relative to those reported for solid or porous PMMA constructs [13,52-57]. Existing antibiotic-releasing PMMA formulations, where antibiotic drugs are directly mixed into the cement, usually feature a poor drug elution profile consisting of a large initial burst release followed by an ineffective slow release over days or weeks. The non-degradable polymer entraps medications in its inner domain with limited accessibility to the exterior for drug diffusion, thus leading to incomplete release of entrapped antibiotics [13, 53-55]. Although the release kinetics can be improved by creating additional elution mechanisms (such as increasing drug loading or incorporating solid porogens to induce porosity), the resulting enhancement in the total amount of drug released is not significant (10-20%) [52,54-57]. The PMMA/CMC/PLGA constructs described here overcome the problems associated with existing antibiotic-releasing PMMA cements resulting in extended periods of high drug concentration and nearly complete drug release. In these PMMA/CMC/PLGA constructs, both the CMC and the PLGA incorporation play essential roles in improving drug release: the rapid CMC dissolution creates open paths for fluid penetration to initiate PLGA polymer hydrolysis; the gradual PLGA degradation controls drug release for a prolonged period and creates further paths for more complete drug release. Eliminating either the PLGA or CMC component did not yield improved drug release, as our previous experiences demonstrated that PLGA microsphere-incorporating solid PMMA constructs (without CMC to impart porosity) exhibited a low initial burst with little or no further release due to the lack of open paths for polymer degradation and drug dissolution; drug-incorporating porous PMMA/CMC constructs (without PLGA microspheres loaded with drugs) exhibited a large initial burst with little or no further release due to the lack of a controlled release mechanism (data not shown).

Notably, the daily colistin release from the PMMA/CMC/PLGA constructs remained at a relatively high level considering that colistin exhibits excellent activity against susceptible species with reported minimum inhibitory concentrations (MICs) of 0.5-5 μg/mL [58-60]. The released colistin presumably created a local concentration well exceeding its inhibitory concentration (e.g., 33-84 fold higher than the MIC of colistin against *Acinetobacter baumannii* at the lowest point of lag phase of day 15) during the release period of 5 weeks (Figure 7B). Antibiotic release at a concentration significantly greater than the MIC has great

potential for rapid bacterial clearing. For these PMMA/CMC/PLGA constructs, both the amount of drug release and the release duration meet the criteria of efficient local antibiotic delivery [32].

The drug release study suggested that impregnating PLGA microspheres into PMMA porous constructs resulted in a similar release pattern as that of PLGA microspheres alone. Potentially, the PMMA/CMC/PLGA constructs developed in this study can serve as a platform of drug-releasing porous implant materials for a wide range of drug delivery applications (e.g., other than antibiotic delivery for infection control, growth factors can be controlled delivered via these constructs to prime the wound site), where the pre-designed drug-releasing PLGA microspheres can be readily impregnated into porous PMMA constructs and a desired drug release pattern (including the release duration, release rate, and total release amount) can be further manipulated by modifying the weight percentages of CMC and PLGA incorporated.

5. Conclusions

An antibiotic-releasing porous PMMA/CMC/PLGA construct was fabricated and characterized towards application as a temporary implant for space maintenance/infection control during the initial step of a two-stage regenerative medicine approach. The CMC hydrogel was incorporated to impart porosity with the aim of anchoring the space maintainer to the surrounding host tissue by soft tissue ingrowth into the pores. The colistin-releasing PLGA microspheres were incorporated to control drug release over a prolonged time period through a degradation-controlled mechanism. It was demonstrated that CMC incorporation created controllable surface/bulk porosity and pore interconnectivity in the constructs. Colistin release, benefiting from the open paths created upon the CMC/PLGA dissolution, achieved a 5-week continuous release, potentially creating a local drug concentration well above the MICs of colistin. The surface/bulk porosity, compressive mechanical properties, and *in vitro* drug release kinetics of the PMMA/CMC/PLGA constructs could be tuned by varying the weight percentages of CMC and PLGA incorporation, offering optimal opportunities to further refine the construct to match a specific clinical application in the two-stage regenerative medicine approach.

Acknowledgments

This work was supported by a grant from the Armed Forces Institute of Regenerative Medicine (W81XWH-08-2-0032). JDK acknowledges support from the Baylor College of Medicine Medical Scientist Training Program (NIH T32 GM07330), Rice Institute of Biosciences and Bioengineering's Biotechnology Training Grant (NIH T32 GM008362), and a training fellowship from the Keck Center Nanobiology Training Program of the Gulf Coast Consortia (NIH Grant No. 5 T90 DK070121-04). The authors also thank Dr. Nagi Damian for stimulating discussions and technical assistance.

List of abbreviations

ANOVA	analysis of variance
CMC	carboxymethylcellulose
FDA	Food and Drug Administration
HPLC	high-performance liquid chromatography
ISO	International Organization for Standardization
MDR	multidrug-resistant
MIC	minimum inhibitory concentration
microCT	microcomputed tomography

MMA	methylmethacrylate
PBS	phosphate buffered saline
PLGA	poly(lactic-*co*-glycolic acid)
PMMA	polymethylmethacrylate
PVA	poly(vinyl alcohol)
SEM	scanning electron microscopy

References

1. Kretlow JD, Young S, Klouda L, Wong M, Mikos AG. Injectable biomaterials for regenerating complex craniofacial tissues. Adv Mater 2009;2:3368–3393. [PubMed: 19750143]
2. Akhlaghi F, Aframian-Farnad F. Management of maxillofacial injuries in the Iran-Iraq war. J Oral Maxillofac Surg 1997;5:927–930. [PubMed: 9294500]
3. Koshima I, Nanba Y, Tsutsui T, Itoh S. Sequential vascularized iliac bone graft and a superficial circumflex iliac artery perforator flap with a single source vessel for established mandibular defects. Plast Reconstr Surg 2004;113:101–106. [PubMed: 14707627]
4. Rodriguez ED, Martin M, Bluebond-Langner R, Manson PN. Multiplanar distraction osteogenesis of fibula free flaps used for secondary reconstruction of traumatic maxillary defects. J Craniofac Surg 2006;17:883–888. [PubMed: 17003616]
5. Thorne CH. Gunshot wounds to the face. Current concepts. Clin Plast Surg 1992;19:233–244. [PubMed: 1537221]
6. Gruss JS, Antonyshyn O, Phillips JH. Early definitive bone and soft-tissue reconstruction of major gunshot wounds of the face. Plast Reconstr Surg 1991;87:436–450. [PubMed: 1998014]
7. Kihtir T, Ivatury RR, Simon RJ, Nassoura Z, Leban S. Early management of civilian gunshot wounds to the face. J Trauma 1993;35:569–575. [PubMed: 8411281]
8. Suominen E, Tukiainen E. Close-range shotgun and rifle injuries to the face. Clin Plast Surg 2001;28:323–337. [PubMed: 11400826]
9. Goodger NM, Wang J, Smagalski GW, Hepworth B. Methylmethacrylate as a space maintainer in mandibular reconstruction. J Oral Maxillofac Surg 2005;63:1048–1051. [PubMed: 16003639]
10. Kretlow JD, Shi M, Young S, Spicer PP, Demien N, Jansen JA, et al. Porous PMMA space maintainers promote soft tissue coverage of clean/contaminated alveolar bone defects. Biomaterials. 2009 submitted.
11. Benoist M. Experience with 220 cases of mandibular reconstruction. J Maxillofac Surg 1978;6:40–49. [PubMed: 274506]
12. Hartman EH, Vehof JW, de Ruijter JE, Spauwen PH, Jansen J. Ectopic bone formation in rats: the importance of vascularity of the acceptor site. Biomaterials 2004;25:5831–5837. [PubMed: 15172495]
13. Webb JCJ, Spencer RF. The role of polymethylmethacrylate bone cement in modern orthopaedic surgery. J Bone Joint Surg Brit Vol 2007;89:851–857.
14. Lewis G. Properties of acrylic bone cement: state of the art review. J Biomed Mater Res 1997;38:155–182. [PubMed: 9178743]
15. Cho YR, Gosain AK. Biomaterials in craniofacial reconstruction. Clin Plast Surg 2004;31:377–85. [PubMed: 15219744]
16. Neovius E, Engstrand T. Craniofacial reconstruction with bone and biomaterials: review over the last 11 years. J Plast Reconstr Aesthet Surg 2009;06:003. 2009. 10.1016/j.bjps
17. Moreira-Gonzalez A, Jackson IT, Miyawaki T, Barakat K, DiNick V. Clinical outcome in cranioplasty: critical review in long-term follow-up. J Craniofac Surg 2003;14:144–153. [PubMed: 12621283]

18. van Mullem PJ, Vaandrager JM, Nicolai JP, de Wijn JR. Implantation of porous acrylic cement in soft tissues: an animal and human biopsy histological study. Biomaterials 1990;11:299–304. [PubMed: 2205300]
19. Bruens ML, Pieterman H, de Wijn JR, Vaandrager JM. Porous polymethylmethacrylate as bone substitute in the craniofacial area. J Craniofac Surg 2003;14:63–68. [PubMed: 12544223]
20. Liu JK, Gottfried ON, Cole CD, Dougherty WR, Couldwell WT. Porous polyethylene implant for cranioplasty and skull base reconstruction. Neurosurg Focus 2004;16:ECP1. [PubMed: 15198501]
21. van Mullem PJ, de Wijn JR, Vaandrager JM. Porous acrylic cement: evaluation of a novel implant material. Ann Plast Surg 1988;21:576–82. [PubMed: 3071237]
22. Hacking SA, Bobyn JD, Toh KK, Tanzer M, Krygier JJ. Fibrous tissue ingrowth and attachment to porous tantalum. J Biomed Mater Res 2000;52:631–638. [PubMed: 11033545]
23. Hospenthal DR, Crouch HK. Infection control challenges in deployed US military treatment facilities. J Trauma 2009;66:S120–1288. [PubMed: 19359955]
24. Sebeny PJ, Riddle MS, Petersen K. Acinetobacter baumannii skin and soft-tissue infection associated with war trauma. Clin Infect Dis 2008;47:444–449. [PubMed: 18611157]
25. Yun HC, Branstetter JG, Murray CK. Osteomyelitis in military personnel wounded in Iraq and Afghanistan. J Trauma 2008;64:S163–168. [PubMed: 18376160]
26. Scott P, Deye G, Srinivasan A, Murray C, Moran K, Hulten E, et al. An outbreak of multidrug-resistant Acinetobacter baumannii-calcoaceticus complex infection in the US military health care system associated with military operations in Iraq. Clin Infect Dis 2007;44:1577–1584. [PubMed: 17516401]
27. Karageorgopoulos DE, Falagas ME. Current control and treatment of multidrug-resistant Acinetobacter baumannii infections. Lancet Infect Dis 2008;12:751–762. [PubMed: 19022191]
28. Falagas ME, Kasiakou SK. Colistin: the revival of polymyxins for the management of multidrug-resistant gram-negative bacterial infections. Clin Infect Dis 2005;40:1333–1341. [PubMed: 15825037]
29. Crane DP, Gromov K, Li D, Soballe K, Wahnes C, Buchner H, et al. Efficacy of colistin-impregnated beads to prevent multidrug-resistant A. baumannii implant-associated osteomyelitis. J Orthop Res 2009;27:1008–1015. [PubMed: 19173261]
30. Li J, Nation RL, Turnidge JD, Milne RW, Coulthard K, Rayner CR, et al. Colistin: the re-emerging antibiotic for multidrug-resistant gram-negative bacterial infections. Lancet Infect Dis 2006;6:589–601. [PubMed: 16931410]
31. Zilberman M, Elsner JJ. Antibiotic-eluting medical devices for various applications. J Control Release 2008;130:202–215. [PubMed: 18687500]
32. Kanellakopoulou K, Giamarellos-Bourboulis EJ. Carrier systems for the local delivery of antibiotics in bone infections. Drugs 2000;6:1223–1232. [PubMed: 10882159]
33. Wu P, Grainger DW. Drug/device combinations for local drug therapies and infection prophylaxis. Biomaterials 2006;27:2450–2467. [PubMed: 16337266]
34. De Wijn JR. Poly(methyl methacrylate)-aqueous phase blends: in situ curing porous materials. J Biomed Mater Res 1976;10:625–635. [PubMed: 947924]
35. Freitas S, Merkle HP, Gander B. Microencapsulation by solvent extraction/evaporation: reviewing the state of the art of microsphere preparation process technology. J Control Release 2005;102:313–332. [PubMed: 15653154]
36. Kline T, Holub D, Therrien J, Leung T, Ryckman D. Synthesis and characterization of the colistin peptide polymyxin E1 and related antimicrobial peptides. J Pept Res 2001;57:175–187. [PubMed: 11298918]
37. International Standard (ISO5833). Implants for surgery - acrylic resin cements. 2002
38. Young S, Bashoura AG, Borden T, Baggett LS, Jansen JA, Wong M, et al. Development and characterization of a rabbit alveolar bone nonhealing defect model. J Biomed Mater Res A 2008;86A:182–194. [PubMed: 17969052]
39. Behnia H, Motamedi MH. Reconstruction and rehabilitation of short-range, high-velocity gunshot injury to the lower face: a case report. J Craniomaxillofac Surg 1997;25:220–227. [PubMed: 9268901]

40. Wang G, Liu SJ, Ueng SW, Chan EC. The release of cefazolin and gentamicin from biodegradable PLA/PGA beads. Int J Pharm 2004;273:203–212. [PubMed: 15010144]
41. Naraharisetti PK, Lew MDN, Fu YC, Lee DJ, Wang CH. Gentamicin-loaded discs and microspheres and their modifications: characterization and in vitro release. J Control Release 2005;102:345–359. [PubMed: 15653156]
42. Ambrose CG, Clyburn TA, Louden K, Joseph J, Wright J, Gulati P, et al. Effective treatment of osteomyelitis with biodegradable microspheres in a rabbit model. Clin Orthop Relat Res 2004;421:293–299. [PubMed: 15123963]
43. Schnieders J, Gbureck U, Thull R, Kissel T. Controlled release of gentamicin from calcium phosphate - poly(lactic acid-co-glycolic acid) composite bone cement. Biomaterials 2006;27:4239–4249. [PubMed: 16620958]
44. Wischke C, Schwendeman SP. Principles of encapsulating hydrophobic drugs in PLA/PLGA microparticles. Int J Pharm 2008;364:298–327. [PubMed: 18621492]
45. Shi XF, Sitharaman B, Pham QP, Liang F, Wu K, Billups WE, et al. Fabrication of porous ultra-short single-walled carbon nanotube nanocomposite scaffolds for bone tissue engineering. Biomaterials 2007;28:4078–4090. [PubMed: 17576009]
46. Thomson RC, Yaszemski MJ, Powers JM, Mikos AG. Fabrication of biodegradable polymer scaffolds to engineer trabecular bone. J Biomater Sci Polym Ed 1995;7:23–38. [PubMed: 7662615]
47. Lin ASP, Barrows TH, Cartmell SH, Guldberg RE. Microarchitectural and mechanical characterization of oriented porous polymer scaffolds. Biomaterials 2003;24:481–489. [PubMed: 12423603]
48. Boger A, Bisig A, Bohner M, Heini P, Schneider E. Variation of the mechanical properties of PMMA to suit osteoporotic cancellous bone. J Biomater Sci Polym Ed 2008;19:1125–1142. [PubMed: 18727856]
49. Barralet JE, Gaunt T, Wright AJ, Gibson IR, Knowles JC. Effect of porosity reduction by compaction on compressive strength and microstructure of calcium phosphate cement. J Biomed Mater Res 2002;63:1–9. [PubMed: 11787022]
50. Vaandrager JM, Vanmullem PJ, Dewijn JR. Porous acrylic cement for the correction of craniofacial deformities and repair of defects, animal experimentation and 2 years of clinical application. Biomaterials 1983;4:128–130. [PubMed: 6860754]
51. Bobyn JD, Wilson GJ, MacGregor DC, Pilliar RM, Weatherly GC. Effect of pore size on the peel strength of attachment of fibrous tissue to porous-surfaced implants. J Biomed Mater Res 1982;16:571–584. [PubMed: 7130213]
52. Frutos P, Diez-Pena E, Frutos G, Barrales-Rienda JM. Release of gentamicin sulphate from a modified commercial bone cement. Effect of (2-hydroxyethyl methacrylate) comonomer and poly(N-vinyl-2-pyrrolidone) additive on release mechanism and kinetics. Biomaterials 2002;23:3787–3797. [PubMed: 12164182]
53. Mader JT, Calhoun J, Cobos J. In vitro evaluation of antibiotic diffusion from antibiotic-impregnated biodegradable beads and polymethylmethacrylate beads. Antimicrob Agents Chemother 1997;41:415–418. [PubMed: 9021200]
54. Mestiri M, Benoit JP, Hernigou P, Devissaguet JP, Puisieux F. Cisplatin-loaded poly(methyl methacrylate) implants - a sustained drug-delivery system. J Control Release 1995;33:107–113.
55. Stevens CM, Tetsworth KD, Calhoun JH, Mader JT. An articulated antibiotic spacer used for infected total knee arthroplasty: a comparative in vitro elution study of Simplex and Palacos bone cements. J Orthop Res 2005;23:27–33. [PubMed: 15607871]
56. van de Belt H, Neut D, Uges DRA, Schenk W, van Horn JR, van der Mei HC, et al. Surface roughness, porosity and wettability of gentamicin-loaded bone cements and their antibiotic release. Biomaterials 2000;21:1981–1987. [PubMed: 10941919]
57. Virto MR, Frutos P, Torrado S, Frutos G. Gentamicin release from modified acrylic bone cements with lactose and hydroxypropylmethylcellulose. Biomaterials 2003;24:79–87. [PubMed: 12417181]
58. Galani I, Kontopidou F, Souli M, Rekatsina PD, Koratzanis E, Deliolanis J, et al. Colistin susceptibility testing by Etest and disk diffusion methods. Int J Antimicrob Agents 2008;31:434–439. [PubMed: 18328674]

59. Lo-Ten-Foe JR, de Smet AM, Diederen BM, Kluytmans JA, van Keulen PH. Comparative evaluation of the VITEK 2, disk diffusion, Etest, broth microdilution, and agar dilution susceptibility testing methods for colistin in clinical isolates, including heteroresistant Enterobacter cloacae and Acinetobacter baumannii strains. Antimicrob Agents Chemother 2007;51:3726–3730. [PubMed: 17646414]

60. Li J, Turnidge J, Milne R, Nation RL, Coulthard K. In vitro pharmacodynamic properties of colistin and colistin methanesulfonate against Pseudomonas aeruginosa isolates from patients with cystic fibrosis. Antimicrob Agents Chemother 2001;45:781–785. [PubMed: 11181360]

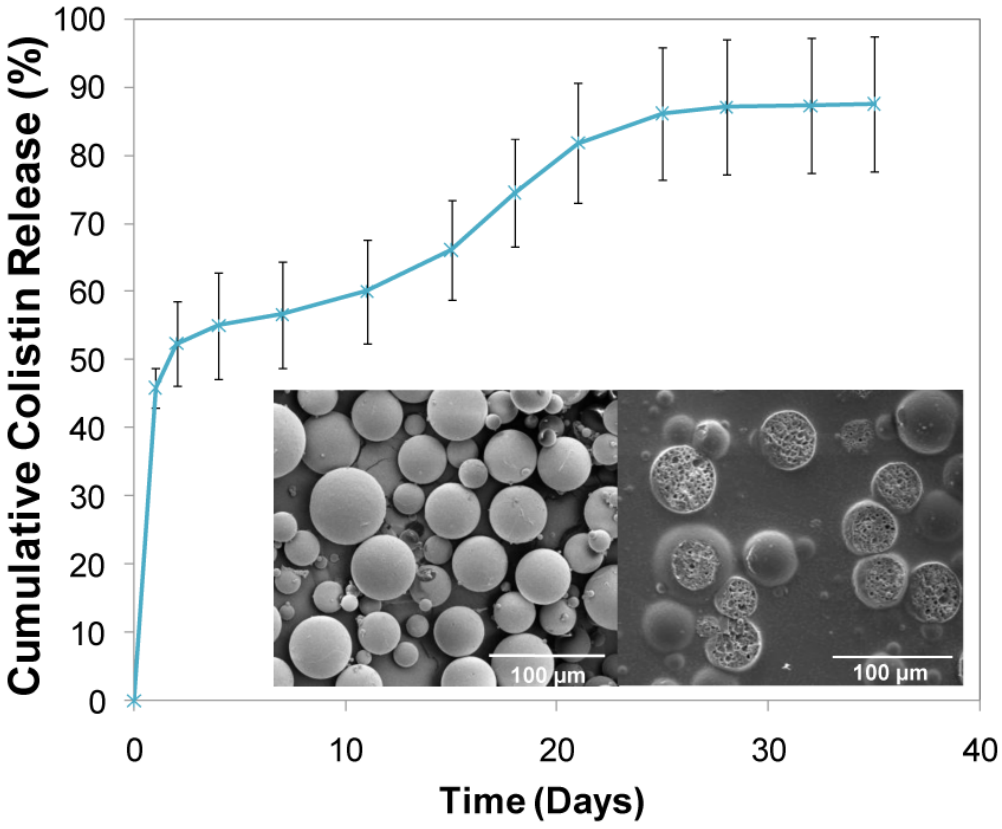

Figure 1.

Cumulative release of colistin from PLGA microspheres: the PLGA microspheres achieved a continuous colistin release over a period of 4 weeks with a total release 87.5±9.9%. The inset pictures show the external (left) and internal (right) morphologies of PLGA microspheres characterized by SEM, where a smooth external surface and porous internal structure of the microspheres are observed. Error bars represent standard deviation for n=3. Size bars are 100 µm.

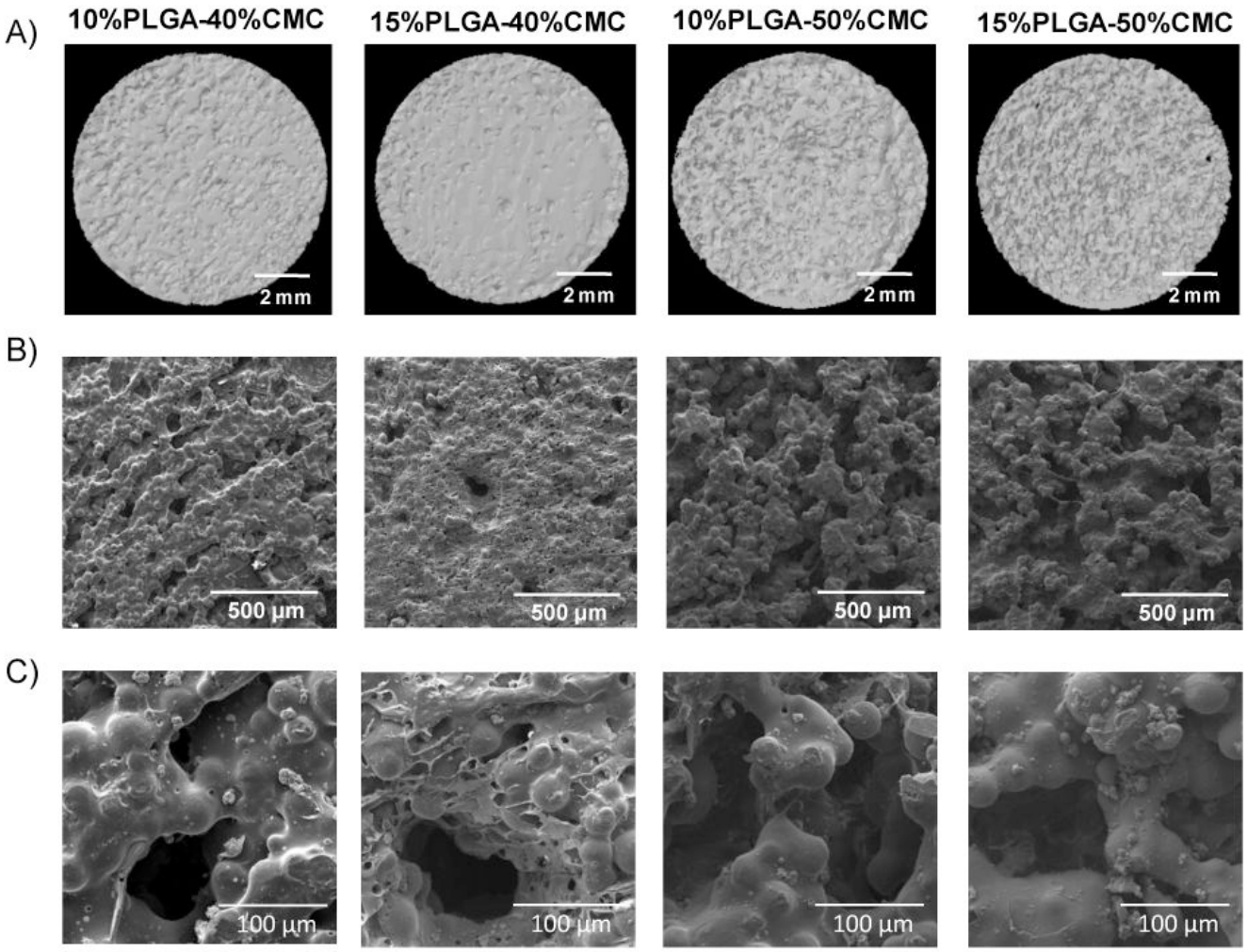

Figure 2.

Surface morphologies of PLGA microsphere-incorporating porous constructs characterized by A) microCT (size bars represent 2 mm); B) SEM (lower magnification, size bars represent 500 µm); and C) SEM (higher magnification, size bars represent 100 µm): surface porosity was created by incorporation of CMC hydrogel, and higher percentages of CMC incorporation led to greater surface roughness.

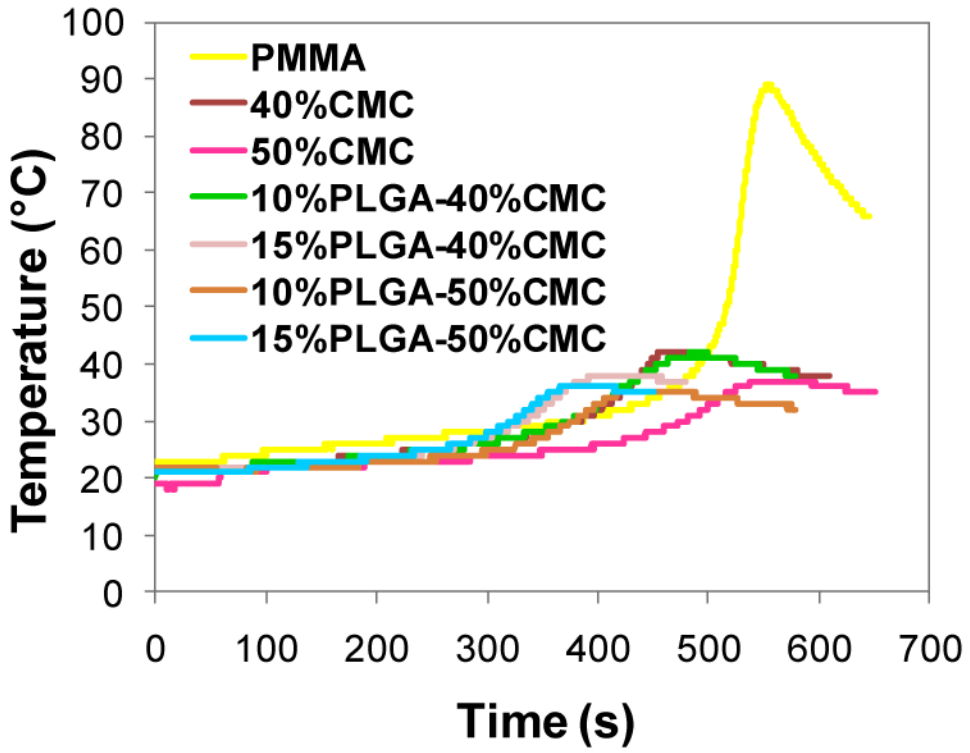

Figure 3.
Representative graphs of temperature change versus time during the setting process of PMMA, PMMA/CMC and PMMA/CMC/PLGA constructs: the maximum temperatures of PMMA/CMC and PMMA/CMC/PLGA constructs attained during the setting process were substantially reduced due to the presence of CMC or CMC/PLGA.

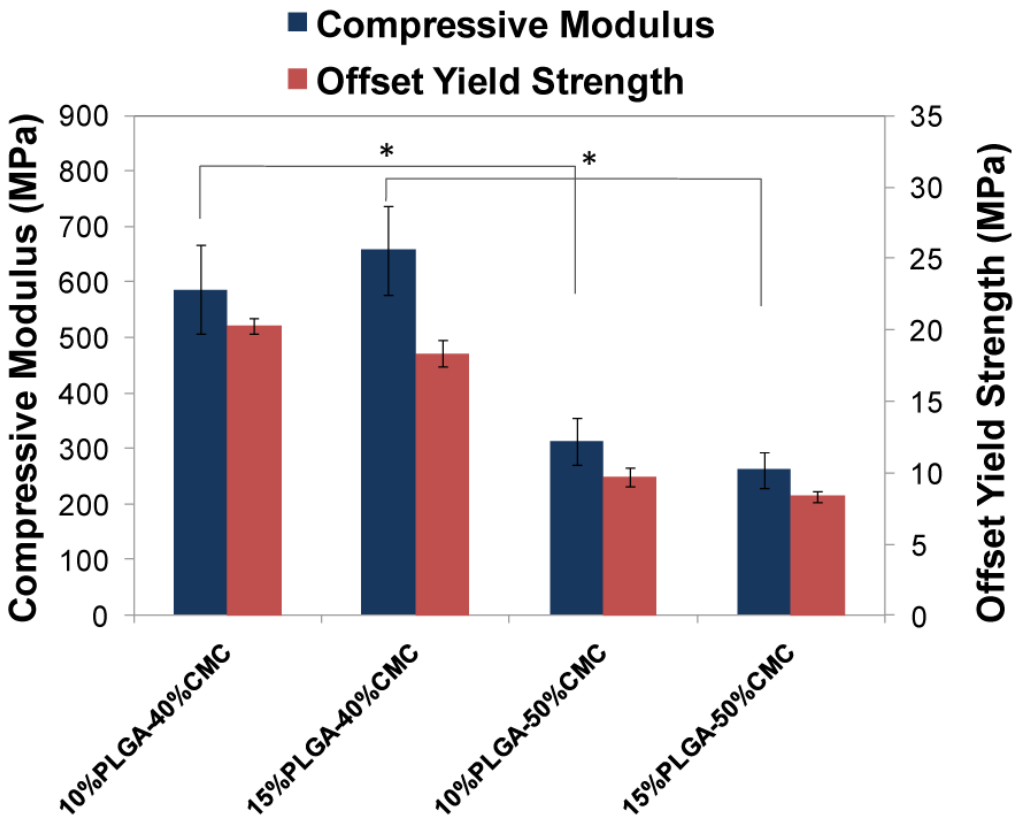

Figure 4.
Compressive modulus and offset yield strength of PMMA/CMC/PLGA constructs: higher CMC incorporation resulted in relatively lower compressive moduli and offset yield strengths. Error bars represent standard deviation for n=6 and statistical significance ($p<0.05$) between relevant groups is denoted by *.

Figure 5A

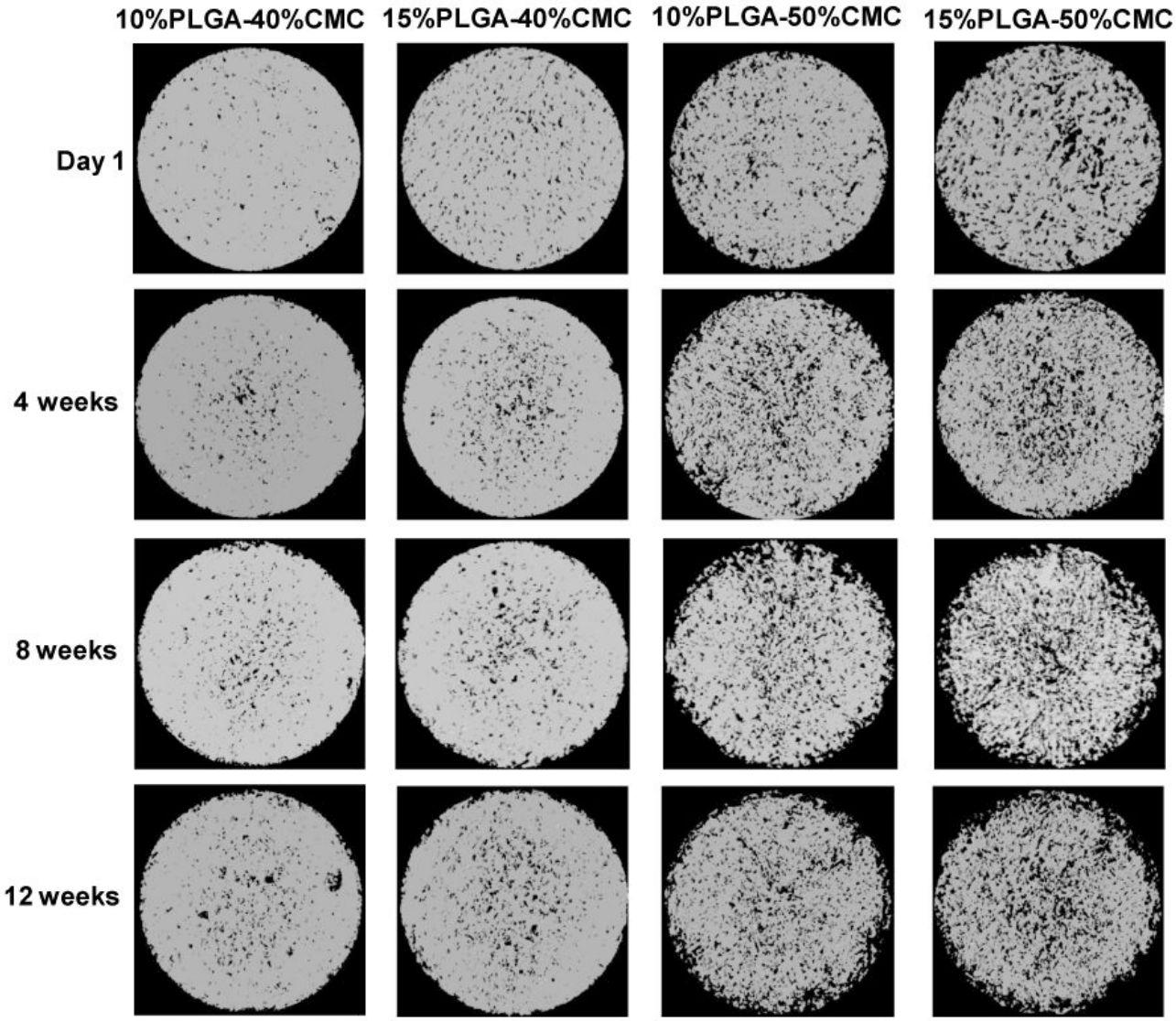

Figure 5B

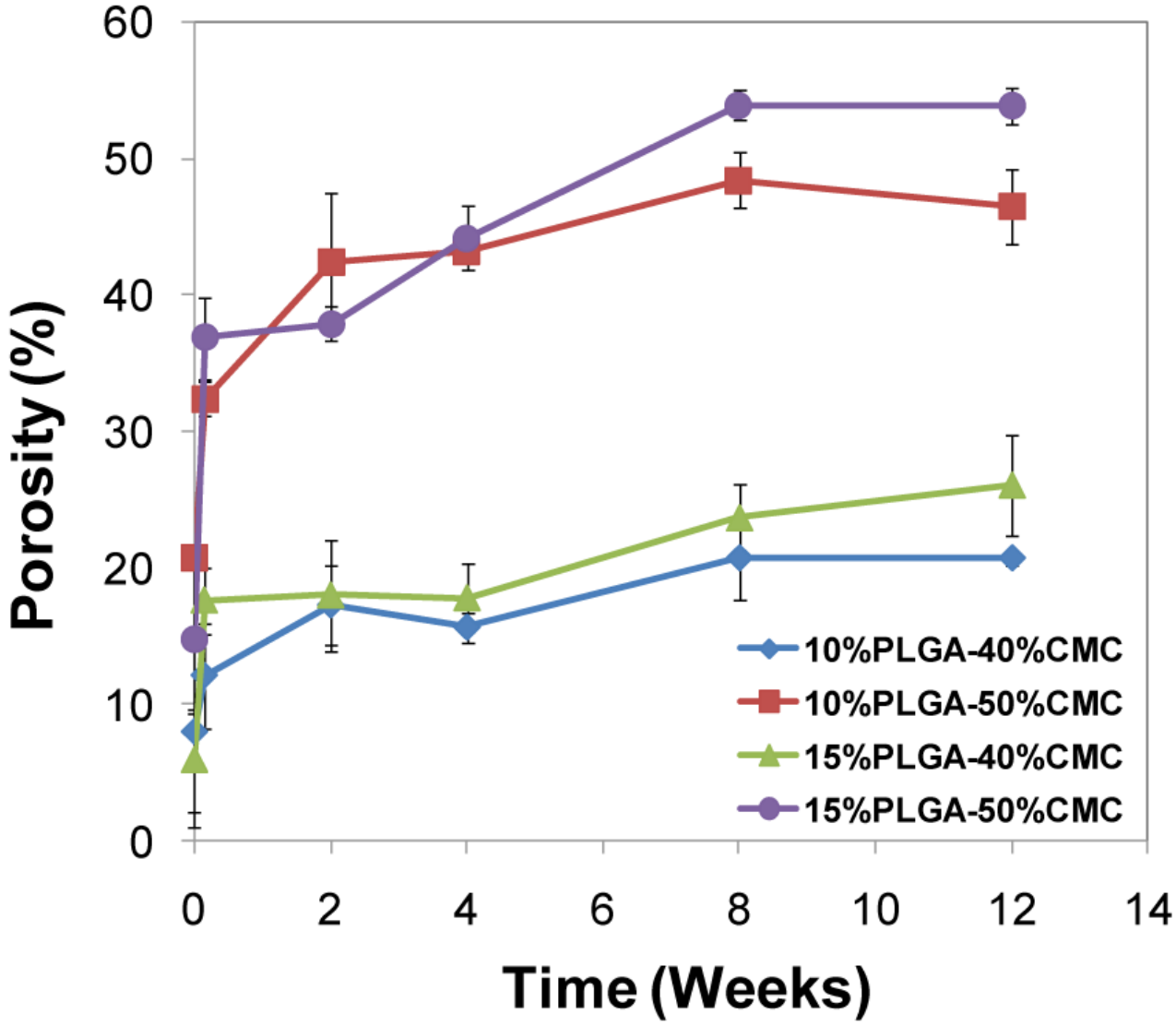

Figure 5C

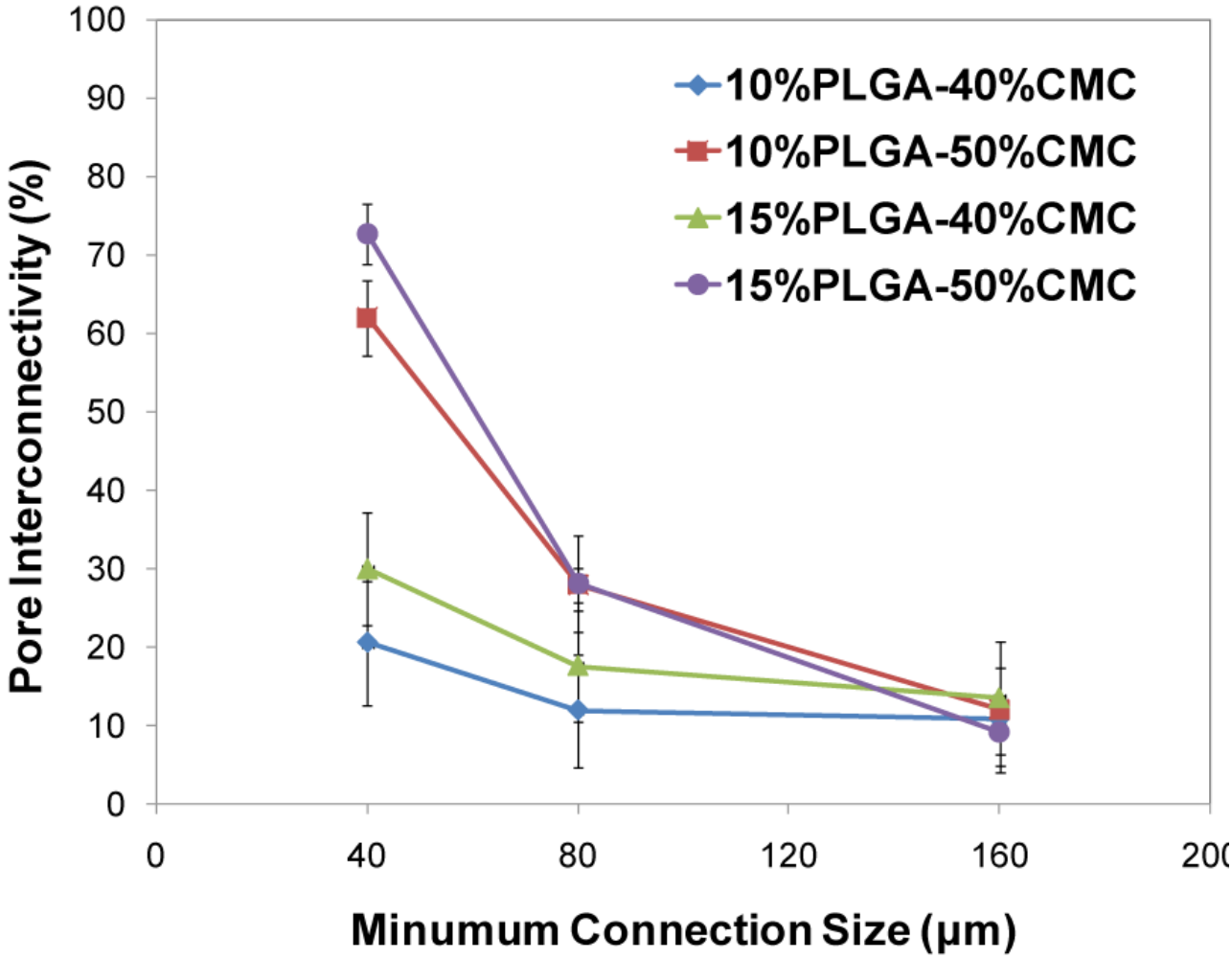

Figure 5.

Degradation of PMMA/CMC/PLGA constructs characterized by microCT: A) Representative 3D reconstruction of cross-sections in the middle of cylindrical constructs (80 μm thickness, top view, size bar represents 2 mm) illustrates increased pores and interconnectivity among pores due to CMC/PLGA component dissolution from the constructs; B) Change of bulk porosity of constructs demonstrated an increased porosity over time. Higher CMC incorporation resulted in greater porosity initially and throughout the degradation process; C) Pore interconnectivity of constructs after one day of degradation was significantly enhanced for the 50 wt% CMC-incorporating construct compared to that of the 40 wt% CMC-incorporating construct at smaller minimum connection sizes. Error bars represent standard deviation for n=3.

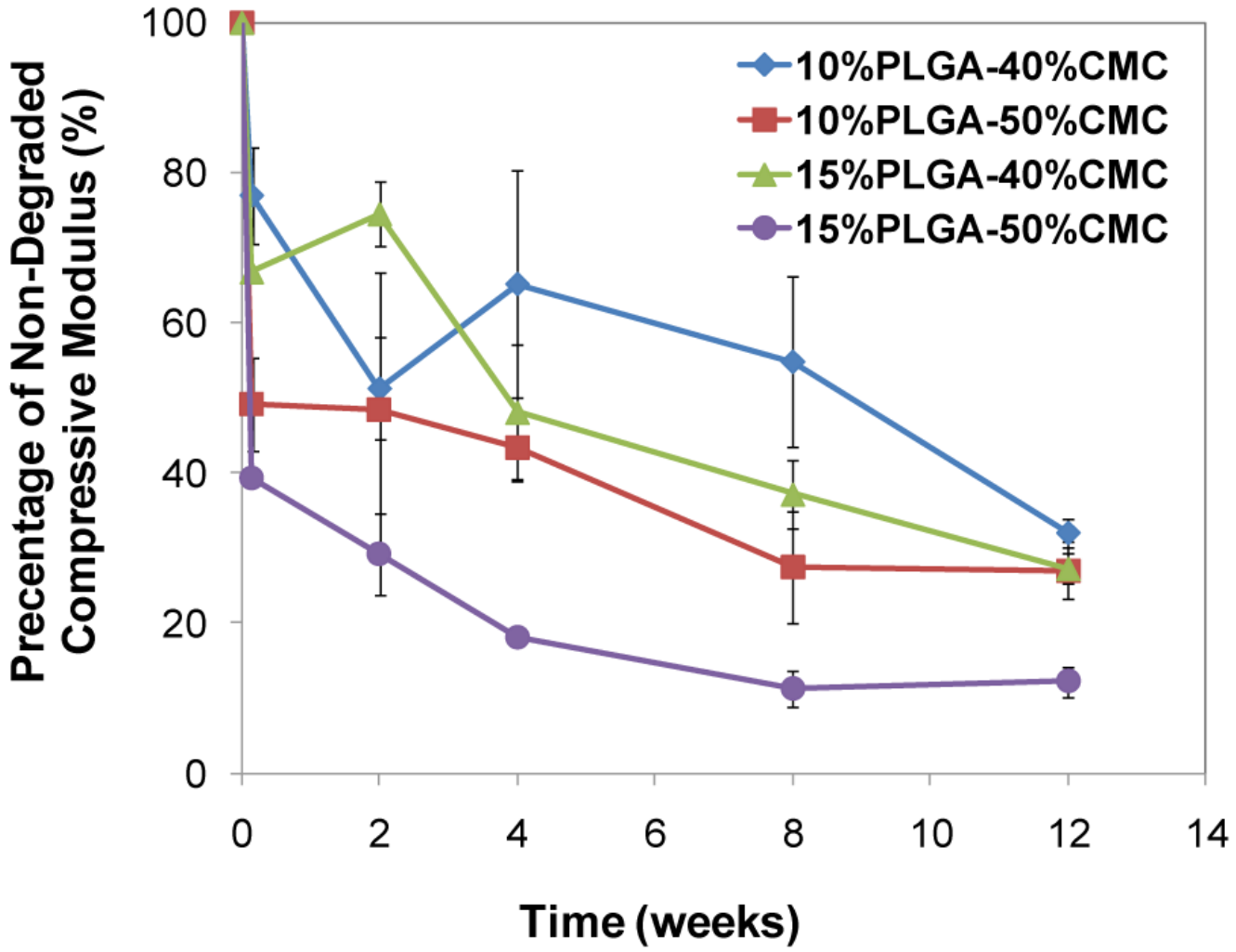

Figure 6.
Change of compressive modulus of constructs during the degradation process, described as a percent of the compressive modulus of the degraded construct over that of the non-degraded construct: the decline of compressive mechanical properties of the cylindrical constructs (10 mm in diameter, 6 mm in height), whose dimension was designed for a mandibular defect model in rabbits, provided predictive insight into the expected mechanical performance of the construct over time *in vivo*. Error bars represent standard deviation for n=3.

Figure 7A

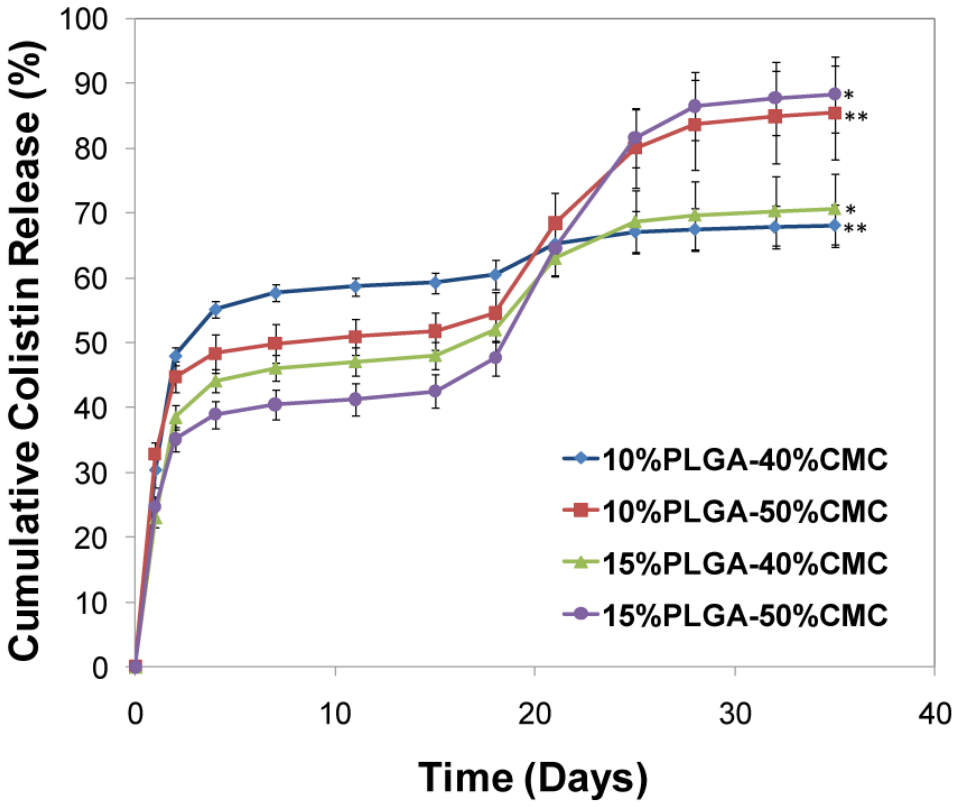

Figure 7B

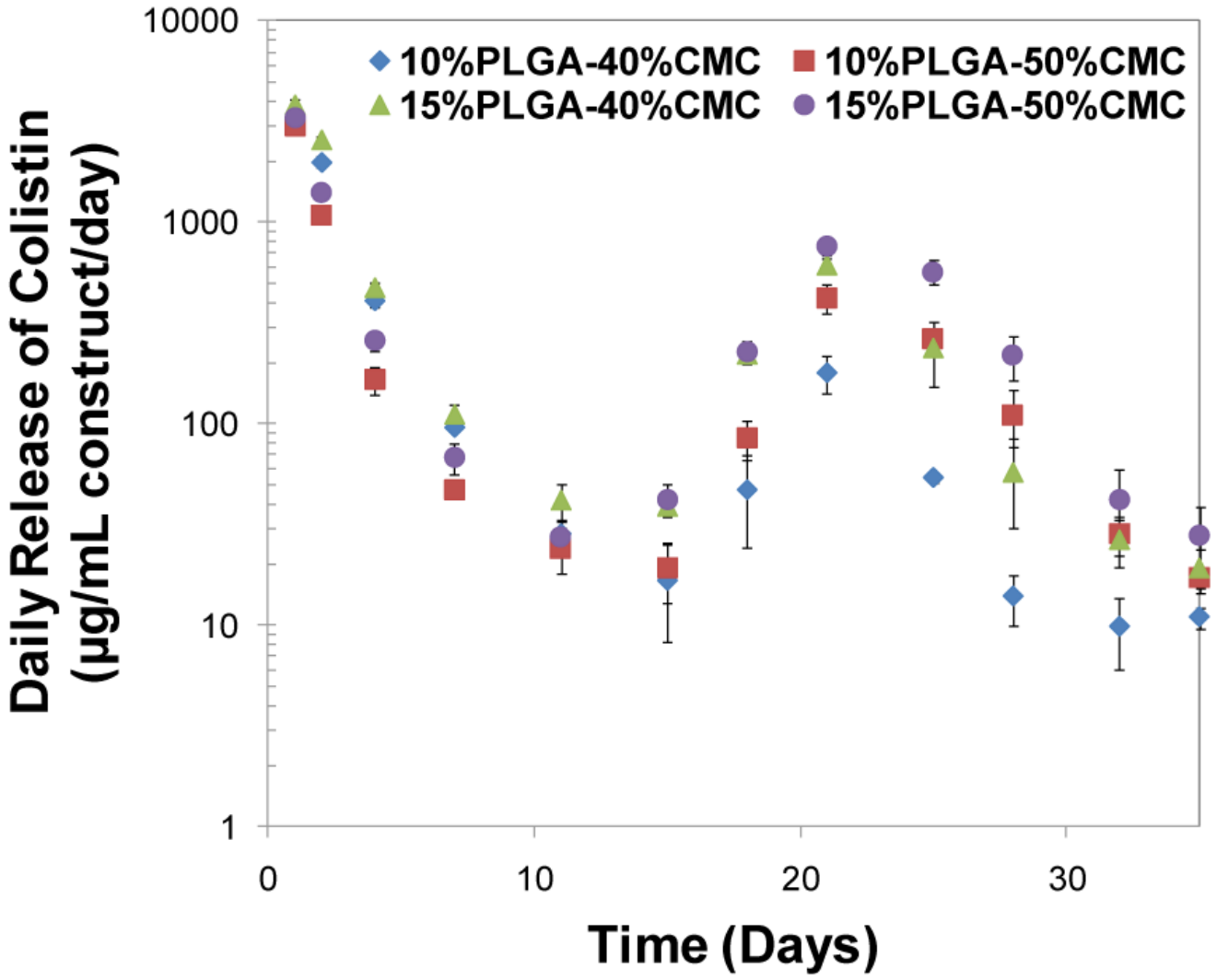

Figure 7.

In vitro colistin release from PMMA/CMC/PLGA constructs: A) The cumulative colistin release from PLGA/PMMA/CMC constructs presented a continuous colistin release over a period of 5 weeks. The total released colistin varied between 68.1±3.3-88.3±5.8% depending on the composition of the construct. Statistical significance between relevant groups is denoted by * and ** ($p<0.05$). B) The daily release of colistin, described as the concentration of released colistin divided by the corresponding release time in days, demonstrated that a constantly high colistin concentration (well above the reported MIC of colistin against its susceptible species) was created via controlled colistin release over 5 weeks. Error bars represent standard deviation for n=3.

Table 1

Composition of microsphere-incorporating PMMA/CMC/PLGA constructs prior to fabrication and in dried samples

PMMA/CMC/PLGA constructs	Initial composition		Composition of dried sample			
	PLGA conc. (wt%)	CMC conc. (wt%)	PLGA conc. (wt%)	CMC salt conc. (wt%)	Drug content	
					(wt%)	mg/mL scaffold
10%PLGA-40%CMC	10	40	9.4	5.7	1.5	11.2
15%PLGA-40%CMC	15	40	14.1	5.7	2.3	16.6
10%PLGA-50%CMC	10	50	9.2	8.3	1.5	9.1
15%PLGA-50%CMC	15	50	13.8	8.3	2.2	13.4

Table 2

Maximum temperature, setting temperature and setting time of various constructs examined

Constructs	Maximum temperature (°C)	Setting temperature (°C)	Setting time (min)
PMMA	88.3±0.6	55.3±0.8	8.4±0.5
40%CMC	43.7±2.1	32.3±1.0	6.7±0.1
10%PLGA-40%CMC	39.3±2.5	29.8±1.0	6.2±0.8
15%PLGA-40%CMC	38.7±1.2	29.8±0.6	5.4±0.2
50%CMC	36.3±1.2	28.3±1.0	7.7±0.3
10%PLGA-50%CMC	34.0±1.0	27.5±0.5	5.7±0.5
15%PLGA-50%CMC	34.7±1.5	28.0±0.5	5.3±0.2

Table 3

Release rates of different phases of colistin release from microsphere-incorporating constructs

PMMA/CMC/PLGA constructs	Phase 1 (day 0-2) (%/day)	Phase 2 (day 2-15) (%/day)	Phase 3 (day 15-28) (%/day)*	Phase 4 (day 28-35) (%/day)	Cumulative release (%)
10%PLGA-40%CMC	24.0±0.7	0.9±0.0	0.6±0.1	0.1±0.0	68.1±3.3#
10%PLGA-50%CMC	22.4±1.2	0.5±0.0	2.5±0.4	0.3±0.0	85.4±7.2#
15%PLGA-40%CMC	19.2±1.0	0.7±0.0	1.7±0.2	0.1±0.0	70.7±5.5##
15%PLGA-50%CMC	17.5±0.9	0.6±0.1	3.4±0.2	0.3±0.1	88.3±5.8##

* In the phase 3 release rates, all groups are statistically different ($p<0.05$).

#, ## indicate the statistical significance ($p<0.05$) between the cumulative release of 10%PLGA-40%CMC and 10%PLGA-50%CMC, and the cumulative release of 15%PLGA-40%CMC and 15%PLGA-50% CMC.